

A comparison of superradiance and negative-phase-velocity phenomenons in the ergosphere of a rotating black hole

Sandi Setiawan*,

School of Mathematics, University of Edinburgh, Edinburgh EH9 3JZ, UK

Tom G. Mackay†, Akhlesh Lakhtakia‡

Department of Engineering Science and Mechanics

Pennsylvania State University, University Park, PA 16802-6812, USA

Abstract

The propagation of electromagnetic plane waves with negative phase velocity (NPV) in the ergosphere of a rotating black hole has recently been reported. A comparison of NPV propagation and superradiance is presented. We show that, although both phenomenons involve negative energy densities, there are two significant differences between them.

Keywords: Negative phase velocity, Superradiance, Poynting vector, Kerr spacetime

1 Introduction

The notion of negative energy is often regarded with suspicion. However, negative energy densities themselves are not uncommon, even within the realm of classical physics [1]. A straightforward example is provided by Newton's law of gravitation. From the perspective of an observer at infinity, negative energy is associated with bound states in the Newtonian gravitational field. Similarly, negative energy is associated with bound states in electrostatics [2].

The concept of negative energy lies at the very heart of quantum mechanics, courtesy of the uncertainty principle. Vacuum fluctuations give rise to manifestations of negative energy density. For example, the so-called squeezed states of light in quantum optics are characterized by periodic spatial distributions of positive and negative energy density [3, 4].

*Fax: + 44 131 650 6553; e-mail: S.Setiawan@ed.ac.uk.

†Corresponding Author. Fax: + 44 131 650 6553; e-mail: T.Mackay@ed.ac.uk; permanent address: School of Mathematics, University of Edinburgh, Edinburgh EH9 3JZ, UK

‡Fax: + 1 814 863 4319; e-mail: akhlesh@psu.edu; also affiliated with Department of Physics, Imperial College, London SW7 2 BZ, UK

Another example is furnished by the Casimir effect, which is a negative-energy phenomenon existing between two closely spaced parallel plates [5, 6, 7].

Negative energy densities are particularly associated with astrophysical settings. Notably, the emission of Hawking radiation by a black hole is accompanied by a flow of negative energy into the black hole [8]. Also, the construction of wormholes — i.e., hypothesized tunnels linking regions of curved spacetime — relies on negative energy density [1, 9].

It is widely known that the region of spacetime immediately surrounding the event horizon of a rotating black hole, namely the ergosphere, supports the negative-energy phenomenon of superradiance [10, 11]. By this process, the extraction of energy from the black hole — via the creation of negative-energy photons within the ergosphere — may be envisaged. Recently, we reported on an unusual form of electromagnetic planewave propagation, called negative phase velocity (NPV) propagation, in the ergosphere of the Kerr black hole [12, 13]. NPV propagation also appears to involve negative energy density [14]. The question naturally arises: are superradiance and NPV propagation related? We address this question in the following sections.

2 Superradiance

Let us briefly review the salient features of black-hole superradiance; comprehensive descriptions can be found elsewhere [10, 11]. We consider the rotating black hole described by the Kerr metric. In Boyer-Lindquist coordinates, the line element in Kerr spacetime is expressed as

$$ds^2 = \frac{\Delta}{\rho^2} (dt - a_{\text{rbh}} \sin^2 \theta d\phi)^2 - \frac{\sin^2 \theta}{\rho^2} [(R^2 + a_{\text{rbh}}^2) d\phi - a_{\text{rbh}} dt]^2 - \frac{\rho^2}{\Delta} dR^2 - \rho^2 d\theta^2, \quad (1)$$

with

$$\Delta = R^2 - 2m_{\text{rbh}}R + a_{\text{rbh}}^2, \quad (2)$$

$$\rho^2 = R^2 + a_{\text{rbh}}^2 \cos^2 \theta. \quad (3)$$

Herein the metric signature $(+, -, -, -)$ is adopted for a black hole of geometric mass m_{rbh} . The term a_{rbh} is a measure of the black hole's angular velocity. The coordinate ϕ is the azimuthal angle around the axis of rotation — which is taken as the z axis of a Cartesian coordinate system — and t is the time coordinate. The coordinate R is related to the Cartesian coordinates (x, y, z) via

$$R^2 = x^2 + y^2 + z^2 - a_{\text{rbh}}^2 (1 - \cos^2 \theta) \quad (4)$$

with $\cos \theta = z/R$.

The outer solution to $\Delta = 0$ corresponds to the outer event horizon of the Kerr black hole; it is denoted by $R = R_+$ where

$$R_+ = m_{\text{rbh}} + \sqrt{m_{\text{rbh}}^2 - a_{\text{rbh}}^2}, \quad (5)$$

with $m_{\text{rbh}}^2 > a_{\text{rbh}}^2$.

For simplicity, let us restrict our attention to the equatorial plane (i.e., $\theta = \pi/2$). The trajectories of photons initially travelling in the $\pm\phi$ direction are provided by

$$\frac{d\phi}{dt} = \frac{g_{t\phi}}{g_{\phi\phi}} \pm \sqrt{\left(\frac{g_{t\phi}}{g_{\phi\phi}}\right)^2 - \frac{g_{tt}}{g_{\phi\phi}}}, \quad (6)$$

where $g_{\alpha\beta}$ are the components of the Kerr metric. Parenthetically, we remark that a central feature of the Kerr black hole is the so-called dragging of inertial frames which results from the off-diagonal metric component $g_{t\phi}$ [15].

From (6) we see that the two solutions

$$\frac{d\phi}{dt} = \begin{cases} \frac{2g_{t\phi}}{g_{\phi\phi}} \\ 0 \end{cases}, \quad (7)$$

emerge for $g_{tt} = 0$. The nonzero solution corresponds to a photon initially travelling in the same directional sense as the black-hole rotation, whereas the zero solution corresponds to a photon initially directed in the opposite sense to the black-hole rotation. Thus, we see that at $g_{tt} = 0$ the frame dragging is sufficiently strong that photon trajectories in the opposite sense to the black-hole rotation are not permitted. The surface where $g_{tt} = 0$ is called the stationary limit surface and it lies at $R = R_{S_+}$ where

$$R_{S_+} = m_{\text{rbh}} + \sqrt{m_{\text{rbh}}^2 - \left(\frac{a_{\text{rbh}}z}{R_{S_+}}\right)^2}. \quad (8)$$

The ergosphere is defined to be the region between the outer event horizon and the stationary limit surface; i.e., the region specified by $R_+ < R < R_{s_+}$.

Since the Kerr spacetime is stationary and axisymmetric, trajectories may be characterized by the following two quantities:

- (i) E , the energy measured at infinity [16], and
- (ii) L , the component of angular momentum parallel to the symmetry axis.

The radial motion of photons travelling in the equatorial plane is described by

$$\left(\frac{dR}{d\sigma}\right)^2 = \frac{(R^2 + a_{\text{rbh}}^2)^2 - a_{\text{rbh}}^2 \Delta}{R^4} (E - V_+) (E - V_-), \quad (9)$$

with

$$V_{\pm} = \left[\frac{2a_{\text{rbh}}m_{\text{rbh}}R \pm R^2\Delta^{1/2}}{(R^2 + a_{\text{rbh}}^2)^2 - a_{\text{rbh}}^2\Delta} \right] L, \quad (10)$$

and σ being an arbitrary parameter on the photon trajectory. It follows thereby that, within the ergosphere, photon trajectories for $a_{\text{rbh}}L > 0$ are characterized by $E > 0$, whereas $E < 0$ solutions exist for $a_{\text{rbh}}L < 0$. That is, the ergosphere supports negative-energy photons provided that their angular momentum is initially directed opposite to the angular momentum of the black hole.

The term superradiance is used to describe the spontaneous emission of positive-energy photons which can take place in the ergosphere of a Kerr black hole [17]. If energy is to be conserved during the emission process [5], the positive energy of the superradiant photons must be balanced by the creation of negative-energy photons.

3 Negative-phase-velocity propagation

The phase velocity of a plane wave is called negative if the wavevector \underline{k} is directed opposite to the time-averaged Poynting vector $\langle \underline{P} \rangle_t$ [18]. Thus, negative-phase-velocity (NPV) propagation is signalled by

$$\underline{k} \cdot \langle \underline{P} \rangle_t < 0. \quad (11)$$

Many interesting consequences follow from (11), most notably the phenomenon of negative refraction [19]. The technological possibilities offered by negative refraction, especially relating to the production of highly efficient lenses, has prompted considerable recent interest in artificial *metamaterials* which support NPV propagation [20]. Furthermore, it has been shown that NPV propagation is possible in vacuum for certain curved spacetime metrics [14].

A brief review of NPV propagation for Kerr spacetime is presented in this section; full details of the analysis are available elsewhere [12, 13]. Following the standard approach, first proposed by Tamm [21], electromagnetic propagation in vacuum for curved spacetime is described in terms of propagation in the fictitious bianisotropic medium characterised by the constitutive relations [22][§]

$$\left. \begin{aligned} D_\ell &= \gamma_{\ell m} E_m + \varepsilon_{\ell mn} \Gamma_m H_n \\ B_\ell &= \gamma_{\ell m} H_m - \varepsilon_{\ell mn} \Gamma_m E_n \end{aligned} \right\}. \quad (12)$$

Herein, $\varepsilon_{\ell mn}$ is the three-dimensional Levi-Civita symbol,

$$\left. \begin{aligned} \gamma_{\ell m} &= -(-g)^{1/2} \frac{g^{\ell m}}{g_{00}} \\ \Gamma_m &= \frac{g_{0m}}{g_{00}} \end{aligned} \right\}, \quad (13)$$

and $g = \det[g_{\alpha\beta}]$. More conveniently, we recast (12) in the conventional 3×3 dyadic/3

[§]Greek indexes take the values 0, 1, 2, and 3 corresponding to t , x , y , and z , respectively; Roman indexes take the values 1, 2, and 3.

vector form

$$\left. \begin{aligned} \underline{D}(ct, \underline{r}) &= \epsilon_0 \underline{\underline{\gamma}}(ct, \underline{r}) \cdot \underline{E}(ct, \underline{r}) - \frac{1}{c} \underline{\underline{\Gamma}}(ct, \underline{r}) \times \underline{H}(ct, \underline{r}) \\ \underline{B}(ct, \underline{r}) &= \mu_0 \underline{\underline{\gamma}}(ct, \underline{r}) \cdot \underline{H}(ct, \underline{r}) + \frac{1}{c} \underline{\underline{\Gamma}}(ct, \underline{r}) \times \underline{E}(ct, \underline{r}) \end{aligned} \right\}, \quad (14)$$

where $\underline{\underline{\gamma}}(ct, \underline{r})$ is the dyadic-equivalent of $\gamma_{\ell m}$, $\underline{\underline{\Gamma}}(ct, \underline{r})$ is the vector-equivalent of Γ_m ; the scalar constants ϵ_0 and μ_0 denote the permittivity and permeability of vacuum in the absence of a gravitational field; $c = 1/\sqrt{\epsilon_0 \mu_0}$; and SI units are adopted.

Planewave propagation has been investigated within an arbitrary spacetime neighbourhood \mathcal{R} whose spatial location is given by the Cartesian coordinates $(\tilde{x}, \tilde{y}, \tilde{z})$ [13]. The neighborhood is taken to be sufficiently small that the nonuniform metric $g_{\alpha\beta}$ may be approximated by the uniform metric $\tilde{g}_{\alpha\beta}$ throughout \mathcal{R} . Thus, we introduce the uniform 3×3 dyadic $\underline{\underline{\tilde{\gamma}}} \equiv \underline{\underline{\gamma}}|_{\mathcal{R}}$ and the uniform 3 vector $\underline{\underline{\tilde{\Gamma}}} \equiv \underline{\underline{\Gamma}}|_{\mathcal{R}}$. Applying standard techniques of planewave analysis within the uniform neighbourhood \mathcal{R} , we previously derived the expression [13]

$$\langle \underline{\mathbf{P}} \rangle_t = \frac{1}{2\omega\mu_0|\underline{\underline{\tilde{\gamma}}}|} \left(|A_a|^2 \underline{\mathbf{e}}_a \cdot \underline{\underline{\tilde{\gamma}}} \cdot \underline{\mathbf{e}}_a + |A_b|^2 \underline{\mathbf{e}}_b \cdot \underline{\underline{\tilde{\gamma}}} \cdot \underline{\mathbf{e}}_b \right) \underline{\underline{\tilde{\gamma}}} \cdot \underline{\mathbf{p}}. \quad (15)$$

for the time-averaged Poynting vector. The vector $\underline{\mathbf{p}}$ in (15) is related to the wavevector $\underline{\mathbf{k}}$ through

$$\underline{\mathbf{p}} = \underline{\mathbf{k}} - \frac{\omega}{c} \underline{\underline{\tilde{\Gamma}}}, \quad (16)$$

with ω being the angular frequency of the plane wave. Furthermore, the corresponding dispersion relation yields two wavenumbers $k = k^\pm$ for the arbitrarily oriented $\underline{\mathbf{k}} = k \hat{\underline{\mathbf{k}}}$ with $\hat{\underline{\mathbf{k}}} = (\sin \theta \cos \phi, \sin \theta \sin \phi, \cos \theta)$, namely,

$$k^\pm = \frac{\omega}{c} \left(\frac{\hat{\underline{\mathbf{k}}} \cdot \underline{\underline{\tilde{\gamma}}} \cdot \underline{\underline{\tilde{\Gamma}}} \pm \sqrt{\left(\hat{\underline{\mathbf{k}}} \cdot \underline{\underline{\tilde{\gamma}}} \cdot \underline{\underline{\tilde{\Gamma}}} \right)^2 - \hat{\underline{\mathbf{k}}} \cdot \underline{\underline{\tilde{\gamma}}} \cdot \hat{\underline{\mathbf{k}}} \left(\underline{\underline{\tilde{\Gamma}}} \cdot \underline{\underline{\tilde{\gamma}}} \cdot \underline{\underline{\tilde{\Gamma}}} - |\underline{\underline{\tilde{\gamma}}}| \right)}}{\hat{\underline{\mathbf{k}}} \cdot \underline{\underline{\tilde{\gamma}}} \cdot \hat{\underline{\mathbf{k}}}} \right). \quad (17)$$

The complex-valued constants $A_{a,b}(\omega/c, \underline{\mathbf{k}})$, which are fixed by initial and boundary conditions, provide the amplitudes accompanying the unit eigenvectors

$$\left. \begin{aligned} \underline{\mathbf{e}}_a &= \frac{\underline{\underline{\tilde{\gamma}}}^{-1} \cdot \underline{\mathbf{w}}}{|\underline{\underline{\tilde{\gamma}}}^{-1} \cdot \underline{\mathbf{w}}|} \\ \underline{\mathbf{e}}_b &= \frac{\underline{\underline{\tilde{\gamma}}}^{-1} \cdot (\underline{\mathbf{p}} \times \underline{\mathbf{e}}_a)}{|\underline{\underline{\tilde{\gamma}}}^{-1} \cdot (\underline{\mathbf{p}} \times \underline{\mathbf{e}}_a)|} \end{aligned} \right\}. \quad (18)$$

The unit vector $\underline{\mathbf{w}}$ is orthogonal to $\underline{\mathbf{p}}$, i.e., $\underline{\mathbf{w}} \cdot \underline{\mathbf{p}} = 0$, but is otherwise arbitrary.

Since

$$|\underline{\underline{\gamma}}| = \delta^2 [R^4 + (a_{\text{rbh}}z)^2]^2 > 0 \quad (19)$$

for the Kerr metric, the sufficient conditions

$$\left. \begin{aligned} (\underline{\underline{\mathbf{e}}}_a \cdot \underline{\underline{\tilde{\gamma}}} \cdot \underline{\underline{\mathbf{e}}}_a) (\underline{\underline{\mathbf{k}}} \cdot \underline{\underline{\tilde{\gamma}}} \cdot \underline{\underline{\mathbf{p}}}) < 0 \\ (\underline{\underline{\mathbf{e}}}_b \cdot \underline{\underline{\tilde{\gamma}}} \cdot \underline{\underline{\mathbf{e}}}_b) (\underline{\underline{\mathbf{k}}} \cdot \underline{\underline{\tilde{\gamma}}} \cdot \underline{\underline{\mathbf{p}}}) < 0 \end{aligned} \right\} \quad (20)$$

for NPV propagation follows directly from (15). In an earlier study, we demonstrated that the NPV sufficient conditions (20) are satisfied for certain wavevector orientations at various locations throughout the ergosphere of the Kerr black hole [13].

4 Superradiance versus NPV propagation

The key feature which is common to both black-hole superradiance and NPV propagation is negative energy: The electromagnetic energy density associated with a NPV plane wave, as observed by an observer at infinity [16], is negative-valued [14, 23]. Negative-energy photon trajectories are required for black-hole superradiance. Furthermore, nonrotating black holes (yielding the Schwarzschild metric by setting $a_{\text{rbh}} = 0$) support neither superradiance nor NPV propagation [13].

However, there are also important differences between these two phenomenons which we now elaborate on.

4.1 Angular momentum considerations

As described earlier, negative-energy photon trajectories arise in the Kerr ergosphere only when a photon's angular momentum is initially directed in the opposite sense to the black-hole rotation. Let us investigate how this compares with the situation for NPV planewave propagation.

The angular momentum density for a plane wave, at the point $\underline{\underline{\mathbf{r}}}$, is provided by $\underline{\underline{\mathbf{r}}} \times \langle \underline{\underline{\mathbf{P}}} \rangle_t$. Furthermore, the component of angular momentum density parallel to the z axis is given as $\underline{\underline{\hat{\mathbf{z}}}} \cdot (\underline{\underline{\mathbf{r}}} \times \langle \underline{\underline{\mathbf{P}}} \rangle_t)$ where $\underline{\underline{\hat{\mathbf{z}}}}$ is a unit vector pointing along the positive z axis. For planewave propagation in the Kerr ergosphere, the sign of $\underline{\underline{\hat{\mathbf{z}}}} \cdot (\underline{\underline{\mathbf{r}}} \times \langle \underline{\underline{\mathbf{P}}} \rangle_t)$ may be inferred using the expression (15) for the time-averaged Poynting vector. Therefore, it can be deduced whether or not NPV plane waves have angular momentum parallel or anti-parallel to the black hole angular momentum.

We present some illustrative numerical results in figures 1 and 2. For the black hole with the angular velocity term $a_{\text{rbh}} = \sqrt{3/4} m_{\text{rbh}}$, we examine three points in the ergosphere, at locations on the x axis given by $R = 1.55 m_{\text{rbh}}$, $R = 1.75 m_{\text{rbh}}$ and $R = 1.95 m_{\text{rbh}}$. Notice that for $a_{\text{rbh}} = \sqrt{3/4} m_{\text{rbh}}$, the outer event horizon lies at $R_+ = 1.5 m_{\text{rbh}}$ whereas the stationary limit surface lies at $R_{S_+} = 2 m_{\text{rbh}}$ on the x axis. In figure 1 the orientations of the NPV wavevectors are mapped. It is observed that the NPV wavevectors generally lie in the

equatorial plane. They are oriented away from the centre of the black hole for the k^+ wavenumbers and oriented towards the centre of the black hole for the k^- wavenumbers. Also, we see that the range of wavevector orientations which support NPV propagation increases as R decreases. The corresponding orientations of the NPV plane wave's angular momentum relative to \hat{z} are mapped in figure 2. We see that for all of the k^+ wavenumbers and some of the k^- wavenumbers, the NPV plane wave's angular momentum is oriented in the opposite direction to the black hole's angular momentum. Most significantly, some of the k^- wavenumbers correspond to NPV planewave angular momentums which are oriented in the same direction as the black hole's angular momentum.

Therefore, we conclude that while many NPV modes may be consistent with the negative-energy photon trajectories of superradiance, there exist NPV modes which are *definitely incompatible* with the superradiant scenario.

4.2 Frequency/wavelength considerations

Black-hole superradiance is a frequency-bounded phenomenon: Superradiance occurs only when [10, 16]

$$\omega < m\omega_+, \quad (21)$$

where $\omega_+ = a_{\text{rbh}}/(2m_{\text{rbh}}R_+)$ is the angular frequency associated with the outer event horizon and $m \geq 1$ is an integer. For spontaneously emitted photons, the probability of large values of m is small.

In contrast, NPV propagation occurs at short wavelengths with no upper bound on frequency. To be specific, suppose that the neighbourhood \mathcal{R} has representative spatial linear dimensions given by ℓ . The approximation of the nonuniform metric $g_{\alpha\beta}$ by the uniform metric $\tilde{g}_{\alpha\beta}$ throughout \mathcal{R} relies upon ℓ being small relative to the radius of curvature of the Kerr spacetime. The inverse radius of spacetime curvature squared is conveniently provided by the nonzero components of the Riemann tensor. For the Kerr metric these components are of the order of R^{-2} [10]. Thus, we have $\ell \lesssim R$. In addition, the neighbourhood \mathcal{R} should be large compared with electromagnetic wavelengths, as given by $2\pi/|k|$. Hence, the NPV conditions (20) hold in the regime

$$\frac{2\pi}{|k|} \lesssim R. \quad (22)$$

5 Concluding remarks

In the introduction, we posed the question: are black-hole superradiance and NPV propagation related? We answer this question as follows. NPV propagation and superradiance are related insofar as both involve negative energy densities within the ergosphere of the Kerr black hole. However, there are two significant distinctions to be made.

- (a) The negative energies in black-hole superradiance are associated with photons which have angular momentum which is initially oriented in the opposite sense to the black-

hole rotation. In contrast, the angular momentum of NPV planewaves can be oriented both in the opposite sense and in the same sense as the black-hole rotation.

- (b) There is practically an upper bound on the frequency of waves which can undergo superradiance. In contrast, NPV propagation occurs at wavelengths which are short relative to the radius of spacetime curvature, but there is no upper bound on frequency.

We conclude by emphasizing that at least two clear differences exist between the phenomena of superradiance and NPV propagation in the ergosphere of a rotating black hole.

Acknowledgements:

SS and TGM acknowledge EPSRC for support under grant GR/S60631/01. TGM thanks the Department of Engineering Science and Mechanics at Pennsylvania State University for their hospitality.

Note added to proof:

The superradiance condition (21) was first established for scalar waves by Starobinsky [24], and for electromagnetic and gravitational waves by Starobinsky and Churilov [25]. From the derivations in these papers, it is clear that superradiance requires the existence of negative energy photons near the black hole event horizon. The authors thank Prof. Starobinsky for drawing their attention to this matter.

References

- [1] C. Barceló, M. Visser, *Class. Quantum Grav.* 17 (2000) 3843.
- [2] D. Halliday, R. Resnick, J. Walker, *Fundamentals of Physics*, 5th Ed., Wiley, New York, USA, 1997.
- [3] R.E. Slusher, L.W. Hollberg, B. Yurke, J.C. Mertz, J.F. Valley, *Phys. Rev. Lett.* 55 (1985) 2409.
- [4] L.H. Ford, T.A. Roman, *Scientific American*, January 2000, pp.46–53.
- [5] L. Spruch, *Science* 272 (1996) 1452.
- [6] S.K. Lamoreaux, *Phys. Rev. Lett.* 78 (1997) 5;
S.K. Lamoreaux, *Phys. Rev. Lett.* 81 (1998) 5475, Corrigendum.
- [7] G. Barton, *J. Phys. A: Math. Gen.* 38 (2005) 2997.
- [8] S.W. Hawking, *Commun. Math. Phys.* 43 (1975) 199.

- [9] M. Safonova, D.F. Torres, G.E. Romero, *Phys. Rev. D* 65 (2001) 023001.
- [10] S. Chandrasekhar, *The Mathematical Theory of Black Holes*, Clarendon Press, Oxford, UK, 1983, Chapter 8.
- [11] B.F. Schutz, *A First Course in General Relativity*, Cambridge Univ. Press, Cambridge, UK, 1985, Chapter 11.
- [12] A. Lakhtakia, T.G. Mackay, S. Setiawan, *Phys. Lett. A* 336 (2005) 89.
- [13] T.G. Mackay, A. Lakhtakia, S. Setiawan, <http://arxiv.org/abs/astro-ph/0501522> (2005).
- [14] T.G. Mackay, A. Lakhtakia, S. Setiawan, *New J. Phys.* 7 (2005) 75.
- [15] J.M. Bardeen, J.A. Petterson, *Astrophys. J.* 195 (1975) L65.
- [16] N. Andersson, B. Jensen, in: E. Pike, P. Sabatier (Eds.), *Scattering*, Academic Press, San Diego, CA, USA, 2002, pp.1607–1626; *gr-qc/0011025*.
- [17] J.D. Bekenstein, M. Schiffer, *Phys. Rev. D* 58 (1998) 064014.
- [18] A. Lakhtakia, M.W. McCall, W.S. Weiglhofer, in: W.S. Weiglhofer, A. Lakhtakia (Eds.), *Introduction to Complex Mediums for Optics and Electromagnetics*, SPIE Press, Bellingham, WA, USA, 2003, pp. 347–363.
- [19] J.B. Pendry, *Contemp. Phys.* 45 (2004) 191.
- [20] S.A. Ramakrishna, *Rep. Prog. Phys.* 68 (2005) 449.
- [21] I.E. Tamm, *Zhurnal Russkogo Fiziko-Khimicheskogo Obshchestva, Otdel Fizicheskii* (J. Russ. Phys.-Chem. Soc, Phys. Section) 56 (1924) 248.
- [22] W. Schleich, M.O. Scully, in: G. Grynberg, R. Stora (Eds.), *New Trends in Atomic Physics*, Elsevier Science Publishers, Amsterdam, The Netherlands, 1984, pp.995–1124.
- [23] R. Ruppin, *Phys. Lett. A* 299 (2002) 309.
- [24] A.A. Starobinsky, *Sov. Phys. JETP* 37 (1973) 28.
- [25] A.A. Starobinsky, S.M. Churilov, *Sov. Phys. JETP* 38 (1973) 1.

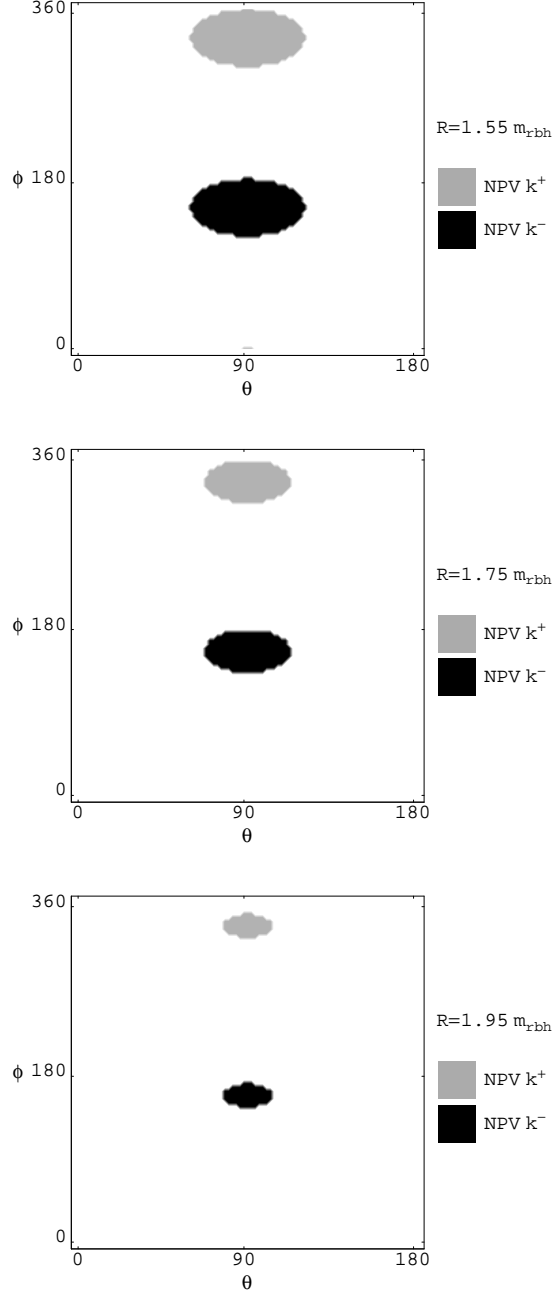


Figure 1: The spherical polar coordinates $\theta \in [0^\circ, 180^\circ)$ and $\phi \in [0^\circ, 360^\circ)$ of the NPV wavevectors at the points on the x axis with $R = 1.55 m_{\text{rbh}}$, $R = 1.75 m_{\text{rbh}}$ and $R = 1.95 m_{\text{rbh}}$, for $a_{\text{rbh}} = \sqrt{3/4} m_{\text{rbh}}$. Note that the outer event horizon lies at $R_+ = 1.5 m_{\text{rbh}}$ whereas the stationary limit surface lies at $R_{S_+} = 2 m_{\text{rbh}}$ on the x axis. Orientations associated with the k^+ and k^- wavevectors are shaded in gray and black, respectively.

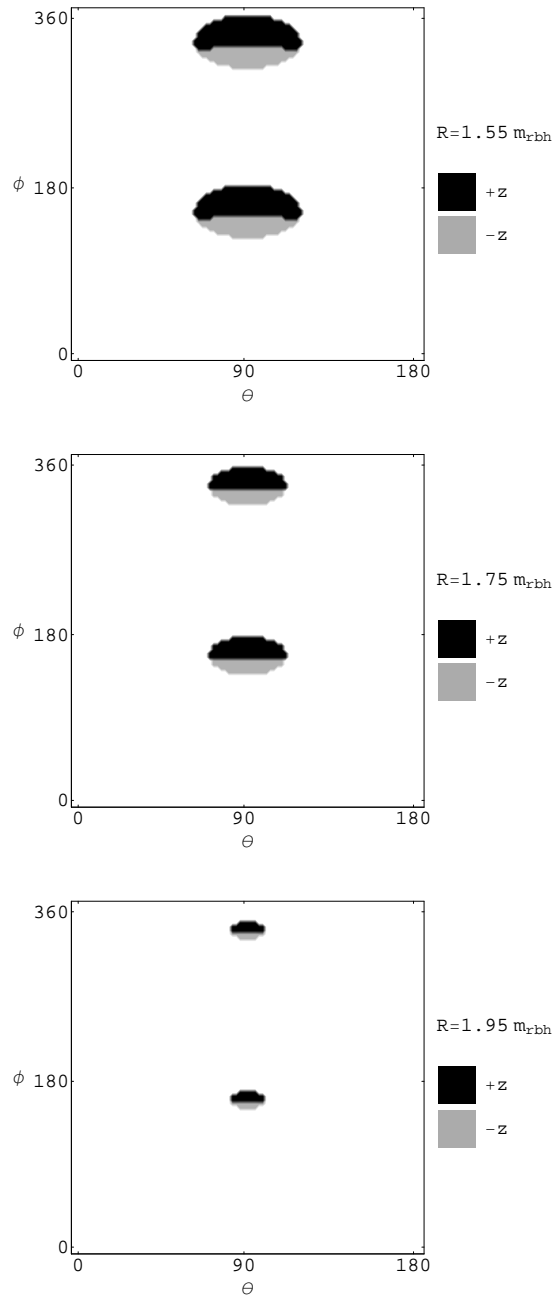


Figure 2: As figure 1 but with wavevector orientations associated with angular momentum in the positive z direction shaded in black and those associated with angular momentum in the negative z direction shaded in gray.